Electronic Supplementary Material (ESI) for RSC Advances.

Supporting Information

Low-Temperature All-Solid-State Lithium-Ion Batteries Based on Di-Cross-Linked Starch Solid Electrolyte

Zehua Lin[a], *Jin Liu*[a]*

[a] School of Metallurgy and Environment, Central South University, Changsha, 410083, P.R. China

AUTHOR INFORMATION

Corresponding Author

* E-mail: jinliu@csu.edu.cn

SUPPORTING FIGURES AND TABLES:

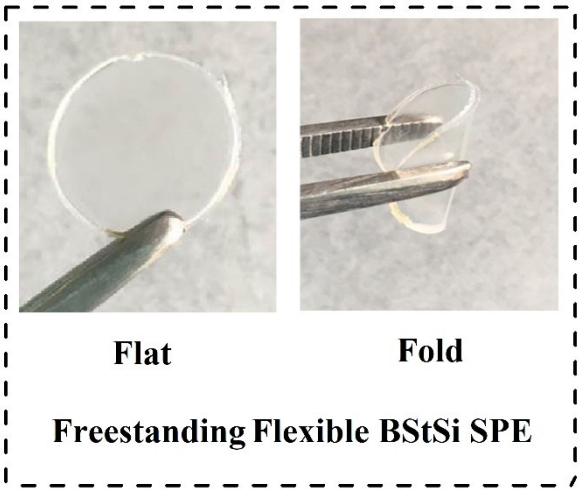

Figure S1. Photos of the flexible and freestanding BStSi SPE films.

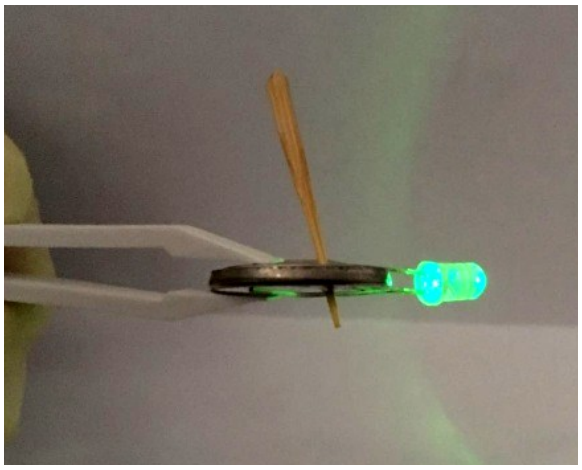

Figure S2. Puncturing experiment of BStSi based ASSLIB

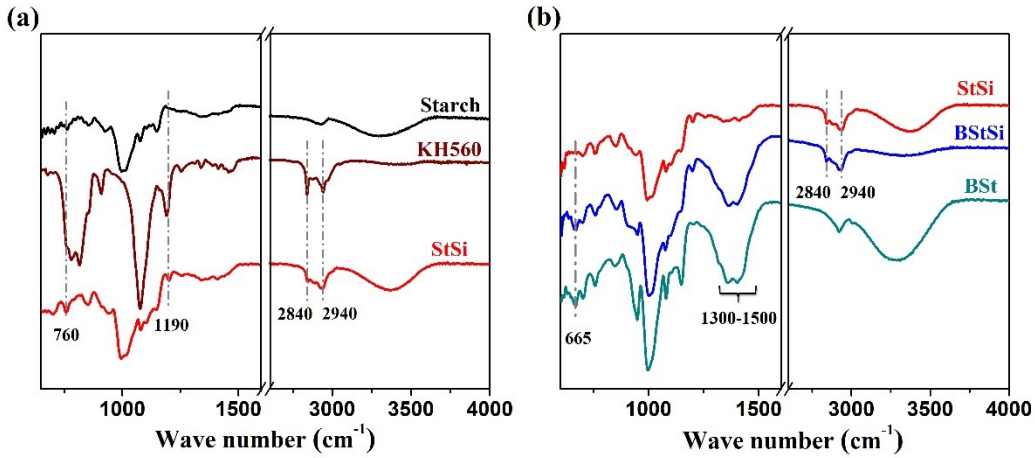

Figure S3. Comparative FTIR of (a) starch, KH560 and StSi and (b) StSi, BStSi and BSt. The range of 2600 cm^{-1} - 1600 cm^{-1} is abbreviated.

FTIR was applied for further confirmation of the reactions among starch and KH560 and BH_3. The spectra of KH560 and StSi from 4000 cm^{-1} to 600 cm^{-1} are shown in Figure S3a. The peak at 1190 cm^{-1} is related to the Si-O-CH_3 groups in KH560 [1]. It decreases evidently in the StSi curve. The characteristic peaks of KH560 at 760 cm^{-1}, belonging to epoxy groups [2], and 2840 cm^{-1} and 2940 cm^{-1}, assigned to methylene [3], are present in the StSi curve, suggesting that the -Si- bonds in KH560 have grafted on starch and the side-product of CH_3OH has been removed.

To verify the reaction between BH_3 and -OH of StSi, the FTIR spectra of BStSi and B-St were also analyzed, which are shown in Figure S3b. Compared to StSi, a new peak of 665 cm^{-1} and a wide peak around 1300~1500 cm^{-1} are seen in the BStSi curve, which are assigned to the B-O bond [4, 5]. This reveals that BH_3 has cross-linked with StSi of the precursor and the BStSi solid electrolyte host forms. The same peaks at 665 cm^{-1} and ~1300 cm^{-1} are also present on the BSt curve, which means the cross-linking reaction occurs between BH_3 and the -OH groups in starch. Further, the hydroxy peak centered at 3430 cm^{-1} is relatively weakened in the BStSi curve compared to that before reaction, revealing that the -OH groups are consumed in the reaction. These results indicate that the synthesis was carried out as designed.

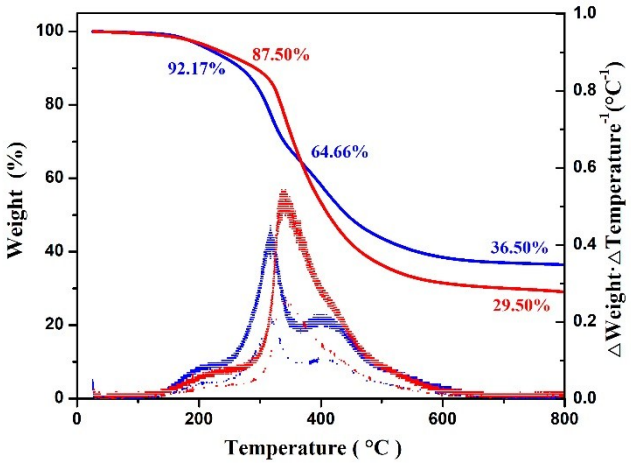

Figure S4. TGA traces of StSi (red) and BStSi (blue) and the derivative thermogravimetric curves of the two samples.

To identify the thermal stability, thermal gravimetric analysis (TGA) is conducted with StSi and BStSi and the results are shown in Figure S4, where the left is the percentage of the sample mass, representing the mass loss, and the right one is the derivative of the mass percentage with respect to temperature, expressing a variation of the weight loss rate. The decomposition temperature of the two samples is higher than 150°C, which is stable enough for the use of ASSLIB below 150°C. From the derivative thermogravimetric curves, the weight loss occurring in the temperature range from 150°C to 250°C corresponds to the decomposition of uncross-linked starch and the hydroxyl dehydration [6]. The weight loss mainly happens between 250°C and 600°C due to the cross-linked product.

There is only one peak in the derivative thermogravimetric curve of StSi, which suggests the decomposition of the product for the KH560 and starch reaction is a one-step decomposition process. [7] Meanwhile, the decomposition of BStSi is a two-step process, including the peaks around 250°C - 350°C and 350°C - 600°C, which can be assigned to the disintegration of two cross-linking forms of Si-Starch and B-Starch.

This two-step decomposition process also confirms that the di-cross-linking reactions of BStSi were completed.

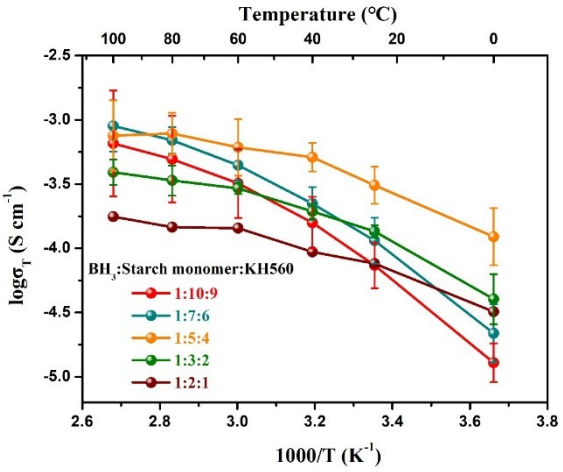

Figure S5. Temperature dependence of the ionic conductivity for the BStSi solid electrolyte at different molar ratios of the components with 50wt% of LiTFSI.

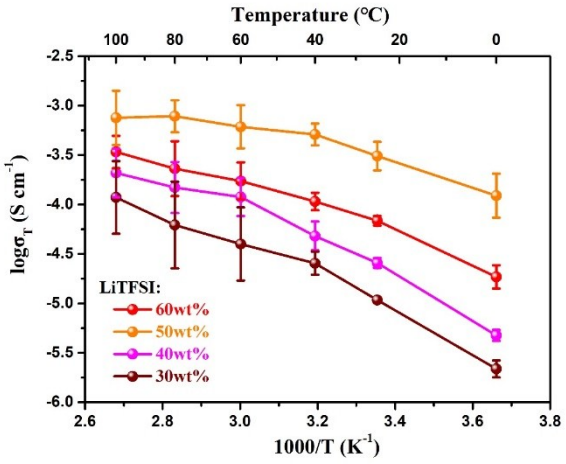

Figure S6. Temperature dependence of the ionic conductivity for the BStSi solid electrolyte at different mass proportions of LiTFSI. The molar ratio of the components is BH_3:Starch monomer:KH560 = 1:5:4.

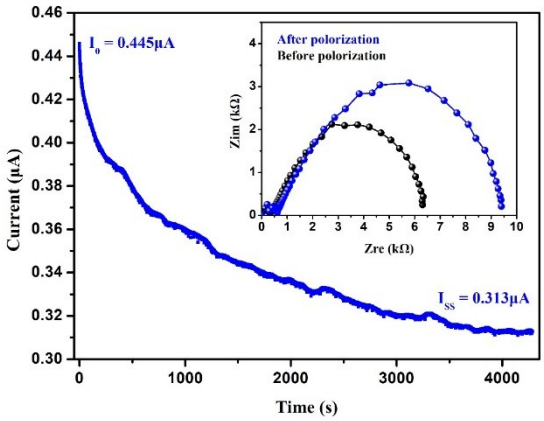

Figure S7. Chronoamperometry of the Li/BStSi/Li cells at -20°C and the inset shows the AC impedance spectra before and after polarization.

Table S1. The t^+ at Different Testing Temperatures and the Relevant Parameters Used for the Calculation of t^+.

25°C		0°C		-20°C	
I_0 = 42.7μA	I_{SS} = 33.2μA	I_0 = 2.11μA	I_{SS} = 1.57μA	I_0 = 0.445μA	I_S =0.313μA
R_0 = 43.4Ω	R_{SS} = 70.5Ω	R_0 = 683Ω	R_{SS} = 1237Ω	R_0 = 5899Ω	R_S = 8765Ω
t^+ = 0.82		t^+ = 0.79		t^+ = 0.72	

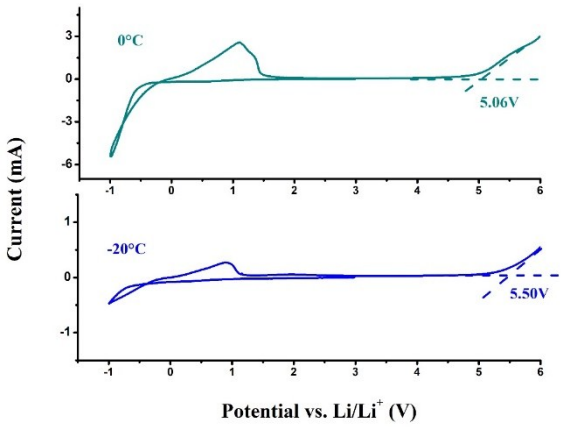

Figure S8. Cyclic voltammetry of the SS/BStSi/Li cells at 0°C and -20°C.

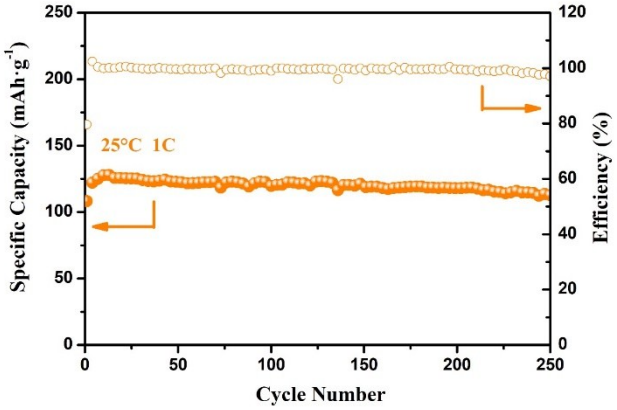

Figure S9. Cycle performance of the LFP/BStSi/Li battery charging/discharging at 25°C and 1C-rate.

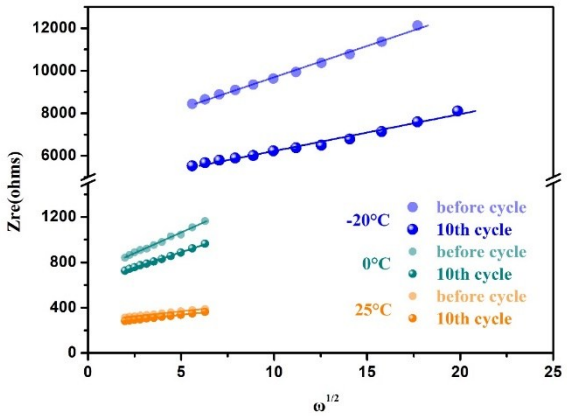

Figure S10. The relationship between Z_{re} and $\omega^{-1/2}$ at the low-frequency region of the LFP/BStSi/Li batteries before cycle and after 10 cycles at 25°C, 0°C and -20°C.

Table S2. Lithium ion diffusion coefficients (D) of the LFP/BStSi/Li batteries before cycle and after 10 cycles at 25°C, 0°C and -20°C and the relevant parameters used for the calculation of D.

Temperature	Cycle	R_b (Ω)	R_{ct} (Ω)	Σ	D (cm^2/s)
25°C	Before cycle	11.0	297	5.75×10^{-2}	2.90×10^{-14}
	10^{th} cycle	9.8	240	5.58×10^{-2}	2.75×10^{-14}

0°C	Before cycle	21.1	954	1.37×10^{-2}	1.37×10^{-15}
	10^{th} cycle	17.4	801	1.85×10^{-2}	2.52×10^{-15}
-20°C	Before cycle	45.7	9638	0.34×10^{-2}	7.28×10^{-17}
	10^{th} cycle	29.1	6241	0.57×10^{-2}	2.09×10^{-16}

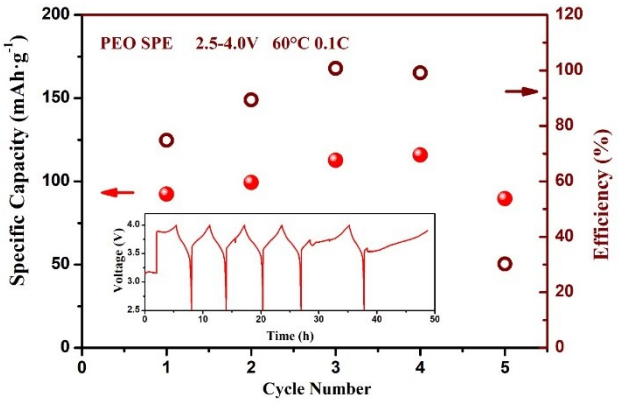

Figure S11. Cycle performance of the NCM811/PEO-LiTFSI/Li battery. The insets illustrate the voltage-time curve during cycling.

REFERENCES

1. Larkin, P. Infrared and Raman spectroscopy: principles and spectral interpretation. Elsevier, 2011.
2. Papke, B.L.; Ratner, M. A.; Shriver, D. F. Vibrational spectroscopy and structure of polymer electrolytes, poly(ethylene oxide) complexes of alkali metal salts. *J. Phys. Chem. Solids*. **1981**. 42(6), 493–500.
3. Yang, Z.; Cai, J.; Zhou, C.; Zhou, D.; Chen, B.; Yang, H.; Cheng, R. Effects of the content of silane coupling agent KH-560 on the properties of LLDPE/magnesium hydroxide composites. *J. Appl. Polym. Sci*. **2010**. 118(5), 2634-2641.
4. Aydın, H.; A. Bozkurt. Synthesis, characterization, and ionic conductivity of novel crosslinked polymer electrolytes for Li-ion batteries. *J. Appl. Polym. Sci*. ***2012***. 124(2), 1193-1199.
5. Uslu, I.; Daştan, H.; Altaş, A.; Yayli, A.; Atakol, O.; Aksu, M. L. Preparation and Characterization of PVA/Boron Polymer Produced by an Electrospinning Technique. *e-Polym*. **2007**. 7(1), 1568.
6. Beninca, C.; Demiate; I. M.; Lacerda, L. G.; Carvalho Filho; M. A. D. S.; Ionashiro, M.; Schnitzler, E. Thermal behavior of corn starch granules modified by acid treatment at 30 and 50 °C. *Eclet. Quím*. **2008**. 33(3): 13-18.

7. Lin, Y.; Li, J.; Liu, K.; Liu, Y.; Liu, J.; Wang, X. Unique starch polymer electrolyte for high capacity all-solid-state lithium sulfur battery. *Green Chem*. **2016**. 18(13), 3796-3803.